Journal Homepage: - www.journalijar.com

INTERNATIONAL JOURNAL OF ADVANCED RESEARCH (IJAR)

Article DOI: 10.21474/IJAR01/11353
DOI URL: http://dx.doi.org/10.21474/IJAR01/11353

ISSN NO. 2320-5407

RESEARCH ARTICLE

COMPARATIVE STUDY OF THE GEOMAGNETIC ACTIVITY EFFECT ON foF2 VARIATION AS DEFINED BY THE TWO CLASSIFICATION METHODS AT DAKAR STATION OVER SEASONS

Sibri Alphonse Sandwidi, Doua Allain Gnabahou and Frédéric Ouattara
Laboratoire de Recherche en Energétique Et Météorologie de l'Espace (LAREME) de l'Université Norbert ZONGO, BP 376 Koudougou Burkina Faso.

Manuscript Info

Manuscript History
Received: 15 May 2020
Final Accepted: 20 June 2020
Published: July 2020

Key words:-
Geomagnetic Activity Classification Method, Ionosphere, foF2 Diurnal Profile, Seasonal Asymmetry

Abstract

The occurrences of the disturbed geomagnetic activities (RA, SA and FA) according to both classifications (AC and NC) have been studied at Dakar ionosonde station (Lat: 14.8°N; Long: 342.6°E). RA occurs more during equinoctial months than during solstices; thus there is a semi-annual asymmetry during RA (which is more marked during the AC). The maximum negative Δ_{occ}, observed during summer, is -16.1% and the maximum positive one, observed during spring, is $+14.73\%$. SA of the AC occurs more during equinoctial times than during solstice periods. Therefore, there is a semi-annual asymmetry; and a winter anomaly is also observed; but, for the NC the SA's occurrence don't differ considerably with the seasons. The maximum negative Δ_{occ}, observed during summer, is -6.08% and the maximum positive one, observed during spring time is $+2.34\%$. During spring and summer, the AC's FA occurrences are greater than those of the NC and we observe the opposite during autumn and winter. The winter and equinoctial anomalies are obviously observed with the FA of the AC; but for those of the NC, we observe an absence of equinoctial anomaly and a slight winter asymmetry. The maximum negative Δ_{occ}, observed during autumn, is -2.75% and the maximum positive one, observed during summer, is $+1.16\%$. The ionosphere F2 layer critical frequency foF2 diurnal profiles throughout seasons concerning both classifications have been compared. The FA diurnal profiles don't show difference over seasons but the RA's and the SA's profiles show an obviousness difference between both classifications during summer time and a non-considerable difference at spring time.

Corresponding Author:- Sibri Alphonse Sandwidi
Address**:-** Laboratoire de Recherche en Energétique Et Météorologie de l'Espace (LAREME) de l'Université Norbert ZONGO, BP 376 Koudougou Burkina Faso.

……..

Introduction:-

The irradiation of the Earth space environment by the magnetized plasma propagating from the Sun induced a continuous global magnetic disturbance namely geomagnetic storms (Legrand and Simon, 1989) In fact, the Sun's magnetic field interacts with the Interplanetary Magnetic Field (IMF) by means of its two components: (1) the poloidal magnetic field which is closed and responsible of the Coronal Mass Ejections (CMEs), the magnetic clouds and high stream solar wind, (2) the toroidal magnetic field named sunspot activities which is the source of slow solar wind (Legrand and Simon, 1989; Richardson et al., 2000, 2001, 2002; Simon and Legrand, 1989).

This Sun-Earth interaction is characterized by four geomagnetic events identified by Legrand and Simon (Legrand and Simon, 1989) by using: (1) the geomagnetic aa index carried out by Mayaud (1971, 1972, 1973, 1980); (2) the date of Sudden Storm Commencement (SSC) and (3) the correlation existing between the geomagnetic aa index and the solar wind speed established by Svalgaard (1977). The same number of geomagnetic activities have been found by Richardson et al. (Richardson et al., 2000, 2001, 2002), but they named the fluctuating activity as the unclear activity which characterized the cases where the solar mechanisms cannot be clearly identified.

This classification gives only 60% of the geomagnetic activities solar sources clarification. Zerbo et al. (2012) established a new classification criteria which clarifies about 80% of the geomagnetic activities solar sources by lowering the limit of the aa index for the shock and recurrent events and adding other causes from solar activity. Then the two schemes are different only for the disturbed geomagnetic activities. This paper deals with the comparison of both classifications critical frequency of the ionosphere F2 layer (foF2) diurnal profiles over seasons as measured at Dakar ionosonde station (Lat: 14.8°N; Long: 342.6°E).

Some papers have been carried out in African Equatorial Ionization Anomaly (EIA) sector about the morphological studies of the foF2 profiles by using Legrand and Simon's classification (Ali et al., 2015; Diabaté et al., 2018, 2019; Gnabahou and Ouattara, 2012; Gnabahou et al., 2013; Guibula et al., 2019; Gyébré et al., 2018; Nanéma and Ouattara, 2013; Nanéma et al., 2019; Nanema et al., 2018; Ouattara, 2013; Ouattara and Amory-Mazaudier, 2012; Ouattara and Nanéma, 2014; Ouattara et al., 2009; Sawadogo et al., 2019a, 2019b; Thiam et al., 2012). Here, we focus our attention to a comparison of both classifications profiles over solar cycle phases on the F2 layer critical frequency (foF2) time variation at Dakar station. The novelty of this study appears as it is a first paper where such comparison is made for both geomagnetic activity classifications methods. This paper aims, in short term, to highlight how the signature of the storm effect is shown by the geomagnetic events of both classifications methods and in mean and long term to contribute to improve the understanding of the sources of geomagnetic activities.

The outline of the paper is as follows: section 2 concerns materials and methods, section 3 is devoted to results and discussions, and the conclusion and research perspectives end the paper as its fourth section.

Data and Method:-

Data:

For the present paper, data involved are: (1) foF2 values carried out at Dakar station. This station operated from 1950 to December 1996. The involved data interval for our study is 1976 – 1995 and concerned Solar Cycle 21 (SC 21) and Solar Cycle 22 (SC 22); (2) Zurich sunspot number (Rz), from OMNI data set http://omniweb.gsfc.nasa.gov/form/dx1.html for the influence of solar cycle phase and (3) Mayaud (1971, 1972, 1973, 1980) geomagnetic index aa for geomagnetic activity impacts. For this study, foF2 diurnal variation are analyzed by considering seasonal impacts. The seasons considered here are: (1) spring (March, April and May); (2) summer (June, July and August); (3) autumn (September, October and November) and (4) winter (December, January and February).

Methods:-

Seasons determination:

The seasons are considered here as: (1) spring (March, April and May); (2) summer (June, July and August); (3) autumn (September, October and November) and (4) winter (December, January and February).

Description of the two geomagnetic activity classification methods:

Based on the strong correlation between geomagnetic index Aa (obtained from the following website: http://isgi.unistra.fr/data_download.php) and solar wind velocity established by Svalgaard (1977), Legrand and Simon

(1989) described criteria for geomagnetic activity classification like this: (1) quiet activity (QA) is characterized by Aa $< 20\ nT$, very quiet activity (VQA) by Aa $< 10\ nT$ and (2) disturbed activities by Aa ≥ 20 nT arranged in three groups such as: (i) recurrent activity (RA) due to solar high wind stream coming from coronal holes with Aa ≥ 40 nT; (2) shock activity (SA) due to Coronal Mass Ejections (CMEs) with Aa ≥ 40 nT and (3) fluctuating activity (FA), consequences of the fluctuation of solar heliosheet.

It's important to note that, this Legrand and Simon's classification or ancient classification (AC) clearly classify only 60% of the geomagnetic activity (Legrand and Simon, 1989; Ouattara and Amory-Mazaudier, 2008, 2009; Ouattara and Zerbo, 2011; Ouattara et al., 2009; Zerbo et al., 2012) whereas the scheme proposed by Zerbo et al. (2012) allows to clearly classify 80% of the geomagnetic activity. The new classification is characterized by: (1) the same limit with the first classification for the quiet activity (Aa $< 20\ nT$) and (2) The lowering of the limit (Aa ≥ 20 nT) for the shock and recurrent events for whom the causes from solar activity are more highlighted (Zerbo et al., 2012). Therefore: (1) recurrent activities (RA), characterised by Aa ≥ 20 nT, are now the recurrent activity of Legrand and Simon plus the Corotative Moderate Activity (CMA) and they are due to solar high wind stream and Corotating interaction Region (CIRs); (2) shock activities (SA) are now the shock activity of Legrand and Simon plus the Cloud Shock Activity (CSA) and they are caused by Coronal Mass Ejections (CMEs) and magnetic clouds, respectively, with Aa ≥ 20 nT and (3) fluctuating activities (FA) or unclear events represent the fluctuating activity of Legrand and Simon plus the Corotating Moderate Activity (CMA); they are consequences of the fluctuation of solar heliosheet. This paper thus concerns the comparison between the profiles of foF2 daily variation during disturbed activities of both schemes of geomagnetic activity classification as described.

The pixel diagram presents the variation of the geomagnetic activity by solar rotation, also called Bartels rotation (Diabaté et al., 2018, 2019; Guibula et al., 2018, 2019; Gyébré et al., 2018; Kaboré et al., 2019; Ouattara et al., 2015, 2017; Ouattara, 2009, 2013; Ouattara and Nanéma, 2014; Ouattara and Zerbo, 2011; Zerbo et al., 2011, 2013). It shows per year an overview of the whole solar geoeffectiveness activity (each type of the solar wind activity [slow, recurrent, CIRs and fluctuating winds activity] and that of CMEs and magnetic clouds (Ouattara and Amory-Mazaudier, 2009). This colour board is used to determine the geomagnetic data as a function of solar activity as described by solar rotation duration (27 days) which consists of: (1) plotting the aa daily values in Bartels diagrams, (2) exhibiting the different types of geomagnetic activities as described above according to both criteria. Figure 2 showed the pixel diagram highlighting the process to determine the different geomagnetic activities following the criteria of the two methods of classification.

Data analysis method:

This paper aims to study the difference of foF2 time variation, throughout the seasons for a given disturbed activity for both geomagnetic activity classifications. The data analysis will be done through two ways: (1) The analysis of the recurrence of the different geomagnetic activities according to both methods of classification over seasons; (2) The profiles obtained are analysed in comparison with the five standard profiles established by Faynot and Vila (1979) for African Equatorial Ionization Anomaly (EIA) region and (3) the quantitative analysis based on comparison between foF2 profiles from both classifications methods.

Firstly, the analysis of the occurrence of the geomagnetic activities is done by: (1) comparing the occurrence of the different geomagnetic activities in relation with both classification by using the equation 1;

$$\Delta_{occ} = GA_{occ} / AC - GA_{occ} / NC \quad (1)$$

Where Δ_{occ} is the gap of the occurrence of the concerning geomagnetic activity classes.
GA_{occ} / AC is the occurrence of the concerning geomagnetic activity class in relation with the ancient classification.
GA_{occ} / NC is the occurrence of the concerning geomagnetic activity class in relation with the new classification.
and (2) putting error bars in data graphs. We can note that error bar is obtained by using the equation 2.

$$\sigma = \sqrt{V} \quad (2)$$

Where V is the variance defined by $V = \frac{1}{N}\sum_{i=1}^{N}(x_i - \bar{x})^2$ with $\bar{x}$ mean value and N the total number of observations for a particular dataset.

Secondly, the foF2 profiles (see Figure 1), linked to the nature, the strength or the absence of electric currents in E layer of ionosphere (Acharya et al., 2010, 2011; Dunford, 1967; Vassal, 1982a, 1982b), are: Noon bite out or "B" profile characterized by a double peak (morning and evening) parted by a trough around midday; Reversed or "R" profile characterized by a single peak at afternoon; Morning pic or "M" profile characterized by a single maximum at

morning; Plateau or "P" profile characterized by an ionization plateau during daytime and Dome profile or "D" profile characterized by a single maximum around noon.

This morphological analysis of the profiles will reveal the difference between the equatorial ionosphere characteristics highlighted by the profiles obtained by both classification methods. In fact those profiles express respectively a signature of a high electrojet, an important afternoon conter-electrojet, a moderate electrojet, a weak electrojet and an absence of electrojet. In addition Fejer, (1981); Fejer et al., (1979, 1981), Abdu et al., (1981, 1992) and Farley et al., (1986) reviewed on mechanism responsible of equatorial trough at noon induced by electrodynamics E × B process.

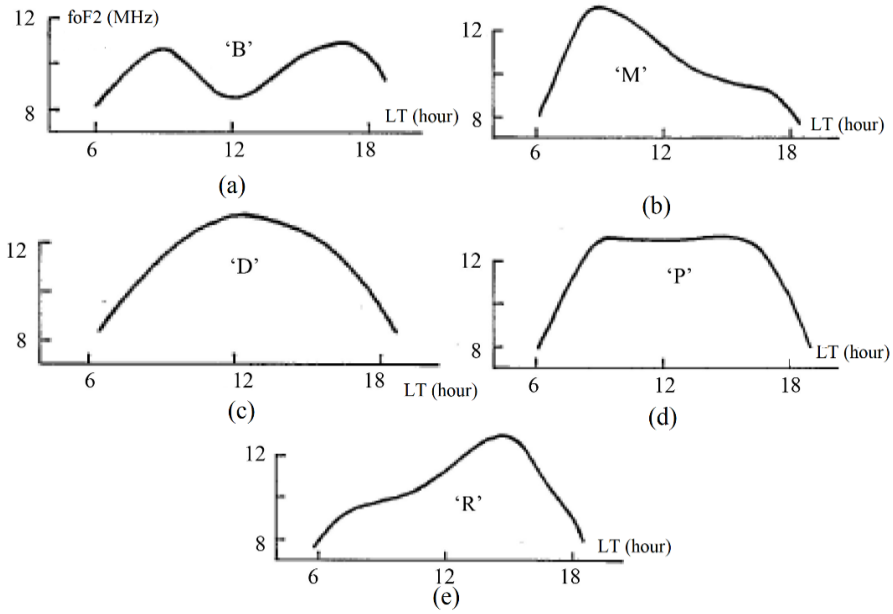

Figure 1:- Faynot and Vila foF2 profile types for African equatorial region. Panel "a" concerns "B" profile that expresses the signature of strong electrojet; panel "b" is "M" profile and exhibits the signature of mean electrojet; panel "c" is "D" and that of panel "d" is "P" profile. These two profiles characterized the absence of electrojet. Panel "e" is "R" profile and expresses the signature of strong counter electrojet.

In a third time, the quantitative analysis based on the appreciation of the difference between foF2 values of the ancient classification and those from the new one will be made through the relative deviation of foF2 defined by:

$$\sigma_{foF2} = \frac{foF2_{AC} - foF2_{NC}}{foF2_{NC}} \times 100 \quad (3)$$

Where $foF2_{AC}$ and $foF2_{NC}$ are the foF2 from the ancient classification and the new one respectively and σ_{foF2} is the relative deviation with the following appreciation:

1. $\sigma_{foF2} > 10\%$ the ancient classification overestimates the new standard classification value;
2. $\sigma_{foF2} < -10\%$ the ancient classification underestimates the new standard classification value;
3. $10\ \% < \sigma_{foF2} < 10\%$ both classifications graphs are in agreement.

Results and Discussion:-

Occurrences of the geomagnetic activities over seasons

Figure 3 highlights the occurrence of the different geomagnetic activities throughout seasons. Panels "a" and "b" concern the classes according to the ancient classification (AC) and the new classification (NC) respectively.

For each season of both classifications, the diagram columns represent respectively the fluctuant, the recurrent, the shock and the very quiet activities. For the occurrence of the fluctuant activity (FA_{occ}) over seasons, we have for the AC, 25.12%; 23.76%; 25.95% and 25.18% and for the NC, 25%; 22.6%; 28.7% and 26.8% respectively for spring, summer, autumn and winter seasons. Therefore, for both classifications, the fluctuant occurs more during the autumn season and less during summer. The maximum negative gap between both classifications occurrences is observed at autumn time with a value $\Delta_{occ} = -2.75\%$ and the maximum positive occurrence is observed in summer season with

a value $\Delta_{occ}= +1.16\%$. Besides, for spring and summer seasons, the FA occurrence of the AC is greater than that of the NC; and we observe the opposite for the autumn and the winter seasons. Consequently, during spring and summer times, the AC's FA occurrences are greater than those of the NC and the opposite is observed during autumn and winter. Winter and equinoctial anomalies are obviously highlighted by the FA of the AC while for those of the NC we observe a less marked winter anomaly and an absence of equinoctial anomaly

For the RA, we have for the AC, 47.43%; 4%; 28.57% and 20% and for the NC, 32.7%; 20.1%, 28.7% and 18.5% respectively for spring, summer, autumn and winter seasons. The recurrent events occur more during the spring season for both classifications; and less during summer for AC and during winter for the NC. The maximum negative gap between both classifications occurrences is observed at summer time with a value of $\Delta_{occ}= -16.1\%$ and the maximum positive occurrence is observed in spring season with a value of $\Delta_{occ}= +14.73\%$. Besides, for spring and winter seasons, the RA's occurrence of the AC is greater than that of the NC; and we observe the opposite for the summer and autumn seasons. Therefore, the RA of the AC occurs more during equinoxes than solstices than the NC's RA; that testify the semi-annual anomaly during RA events which is more marked for the AC.

For the SA, we have for the AC, 27.74%; 19.52%; 26.37% and 26.37% and for the NC, 25.4%; 25.6%; 25.5% and 24.6% respectively for spring, summer, autumn and winter seasons. For the AC, the shock events occur more during the spring, the autumn and the winter seasons with an occurrence included between $[26\%; 28\%]$; and less during the summer with an occurrence of 19.52%. And for the NC, we have a value of occurrence close to 25% for all the seasons. The maximum negative gap between both classification occurrences is observed at summer time with $\Delta_{occ}= -6.08\%$ and the maximum positive one is observed in spring season with $\Delta_{occ}= +2.34\%$. Besides, for summer season, the SA's occurrence of the AC are lower than that of the NC; and we observe the opposite for the other seasons. Therefore, we observe that the AC's SA more occur during equinoxes than solstices; but for those of the NC, there is not an obvious difference between both seasons. In consequence, there is semi-annual anomaly, winter anomaly (due to the asymmetry between winter and summer) and the absence of equinoctial anomaly (due to the fact that the occurrences of spring and autumn season of the AC's SA don't show remarkable difference); that is not the case of the NC because the occurrences of the NC's SA don't differ considerably over seasons..

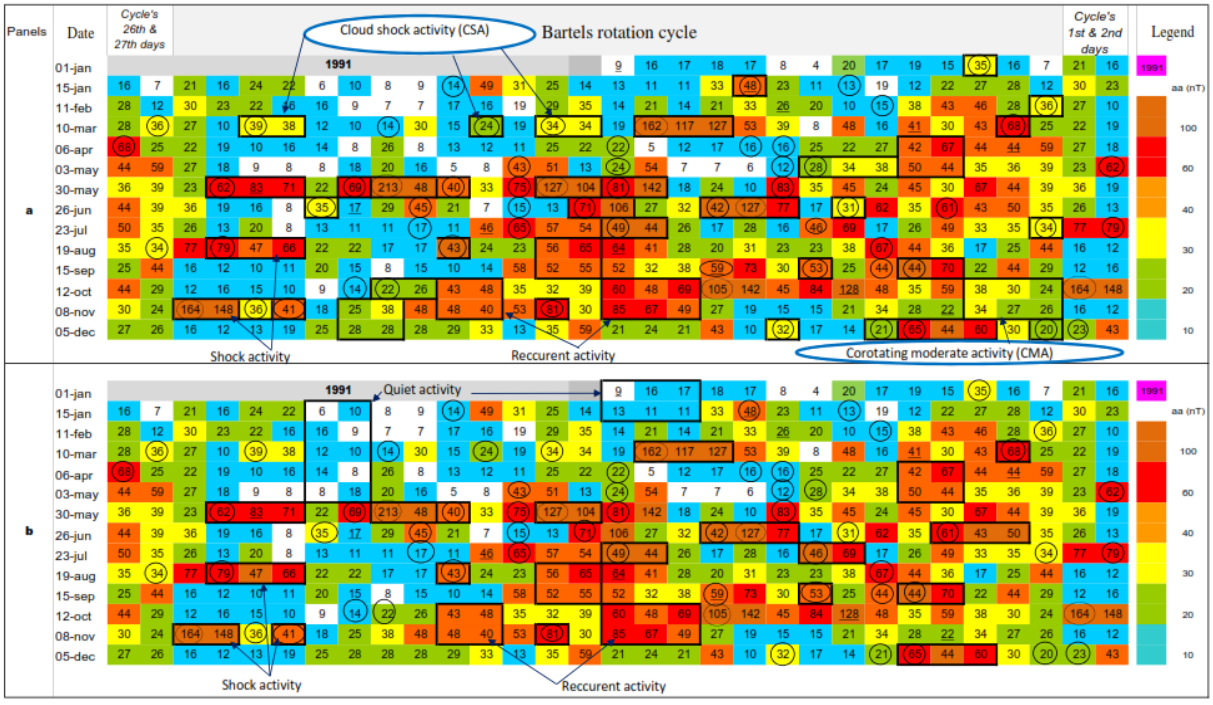

Figure 2:- Pixel diagram used to determine geomagnetic activity classes by the criteria of the ancient classification or AC (panel "b") and the new classification or NC (panel "a"). The blue and white color cases correspond to the quiet activity. The recurrent and the shock activities are those of the AC recurrent and shock events respectively.

The NC recurrent events are those of the AC plus the corotating moderate activity (CMA) and its shock events correspond to those of the AC plus the cloud shock activity.

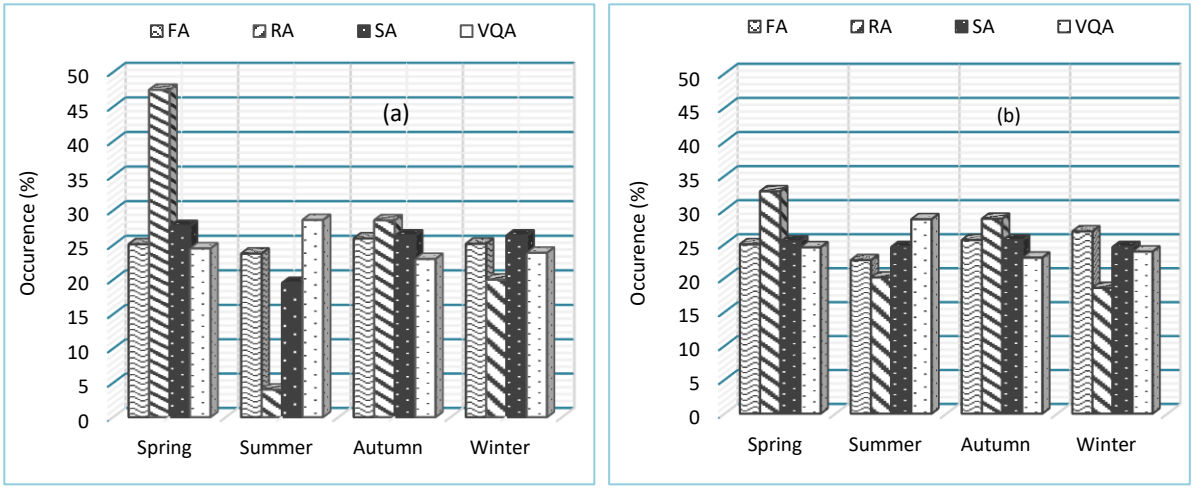

Figure 3:- Comparison of the occurrence of the geomagnetic activity throughout seasons between the Ancient classification (panel "a") and the new classification (panel "b").

Profiles comparison for both classifications throughout seasons:

Figure 4 to Figure 6 show the foF2 profiles during fluctuant activity (FA), recurrent activity (RA) and shock activity (SA) respectively. The panels "a", "b", "c" and "d" present the graph of the spring, summer, autumn and winter seasons respectively. For all geomagnetic activities, the absence of equinoctial asymmetry is clearly highlighted and the figures show this results as those founded by Ouattara et al., (2017) at Niamey station and Guibula et al., (2018) at Korogho station.

Figure 4 shows that, during FA, both graphs show an "R" profile during all seasons but it shows a "M" profile for winter season. Therefore, the FA is characterised by a moderate electrojet during winter season, while it shows an important afternoon conter-electrojet in E layer of ionosphere during the other seasons. The two classification's curves show the same shape and the same amplitude for all seasons with respect to error bars shown in NC graph; thus, for FA the foF2 profiles of the AC and NC don't show difference during all seasons; it is so not important to estimate the relative deviation of foF2 during FA. This absence of difference between the two classifications can be explain by the fact that the FA is characterised by the unclear solar activity; perhaps the highlighting of the twenty percent (20%) of the geomagnetic activity which are mixed in the unclear activities (remember that the NC explain about 80% of the solar activity in relation of the geomagnetic activity) will enable to make difference with the AC.

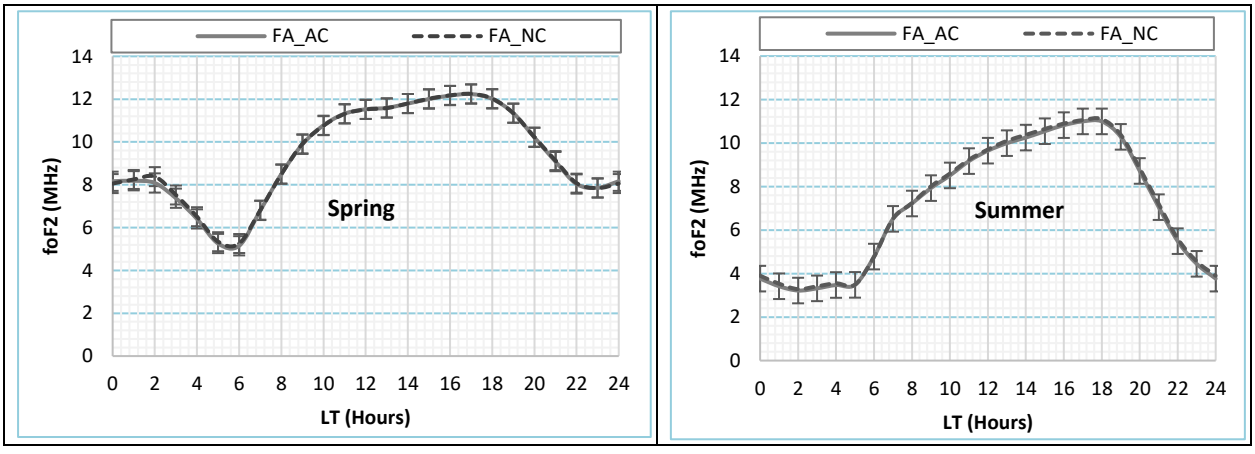

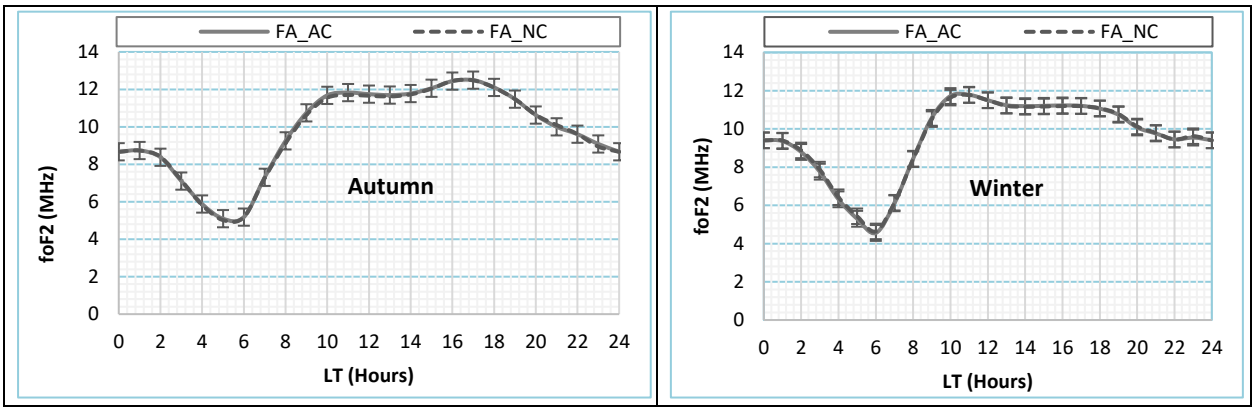

Figure 4:- foF2 profiles during fluctuant geomagnetic activity (FA) during spring, summer, autumn and winter seasons. The dashed curve is for the New classification (NC) and the solid one for the Ancient Classification (AC).

Figure 5 shows the foF2 values' diurnal variation for the RA according to the two classification and the relative deviation percentage of both classifications foF2 values. For equinox seasons (see panels "a" and "c"), the two classification's curves show an "R" profile, with the same shape and the same amplitude with respect to error bars shown in NC graph. Therefore, the RA is characterised by a moderate electrojet during equinox seasons. Otherwise we observe a difference between both classifications curves in the meantime surrounding 0200 LT during spring months and in the meantime surrounding 0700 LT, 2100 LT and 0000 LT concerning autumn season. The right column of the panels "a" and "c" highlight this observation. In fact, for the spring season (panel "a"), the σfoF2 shows value within $\pm 10\%$ between all the time excepted in the meantime surrounding 0200 LT with a maximum negative value of -6.9% observed at 0800 LT and a maximum positive value of 21.55% observed at 0200 LT. And the graph of right column of the panel "c" present a σfoF2 value within $\pm 10\%$ between all the times excepted in the meantime surrounding 0700 LT, 2100 LT and 0000 LT; with a maximum positive value equal to $+13{,}96$, observed at 0000 LT and a maximum negative value equal to $-10{,}28$, observed at 0700 LT.

For the summer month (panel "b") we observe an obviousness difference between both curves; in fact, while we have an "R" profile for the NC, the AC curve show a "B" profile characterised by a late morning peak at about 1400 LT (~10.82 MHz), an afternoon peak at 1800 LT (~11.80 MHz), and a trough at 1500 LT (~9.87 MHz). The obviousness difference between the AC and the NC curves during summer season can also be explain by the large gap ($\Delta_{occ} = -16.1\%$) between the occurrences of the RA for both classifications as shown at the paragraph 3.1. Besides, the right column of this panel highlights a σfoF2 value within $\pm 10\%$ just between after 0600 LT to after 0800 LT and between 1400 LT to 1600 LT; but for the remaining time, σfoF2 values are greater than $+10\%$ or small than -10%. Therefore both classification's RA present an almost different profile during summer season, except between after 0600 LT to after 0800 LT and between 1400 LT to 1600 LT with respect to the σfoF2 value. Panel d shows an "M" profile for both classifications curves during the winter month; therefore the RA profile highlights a moderate electrojet during winter time. Otherwise, we observe a difference between the two graphs after 1700 LT to before 0600 LT with respect to error bars shown in NC graph. Besides, the right column of this panel highlights a σfoF2 value greater than $+10\%$ between 2000 LT to 0600 LT and a value within $\pm 10\%$ the time remaining. The maximum positive value, equal to $+15{,}62$, is observed at 0500 LT and the maximum negative value, equal to $-1{,}59$, is observed at 0800 LT.

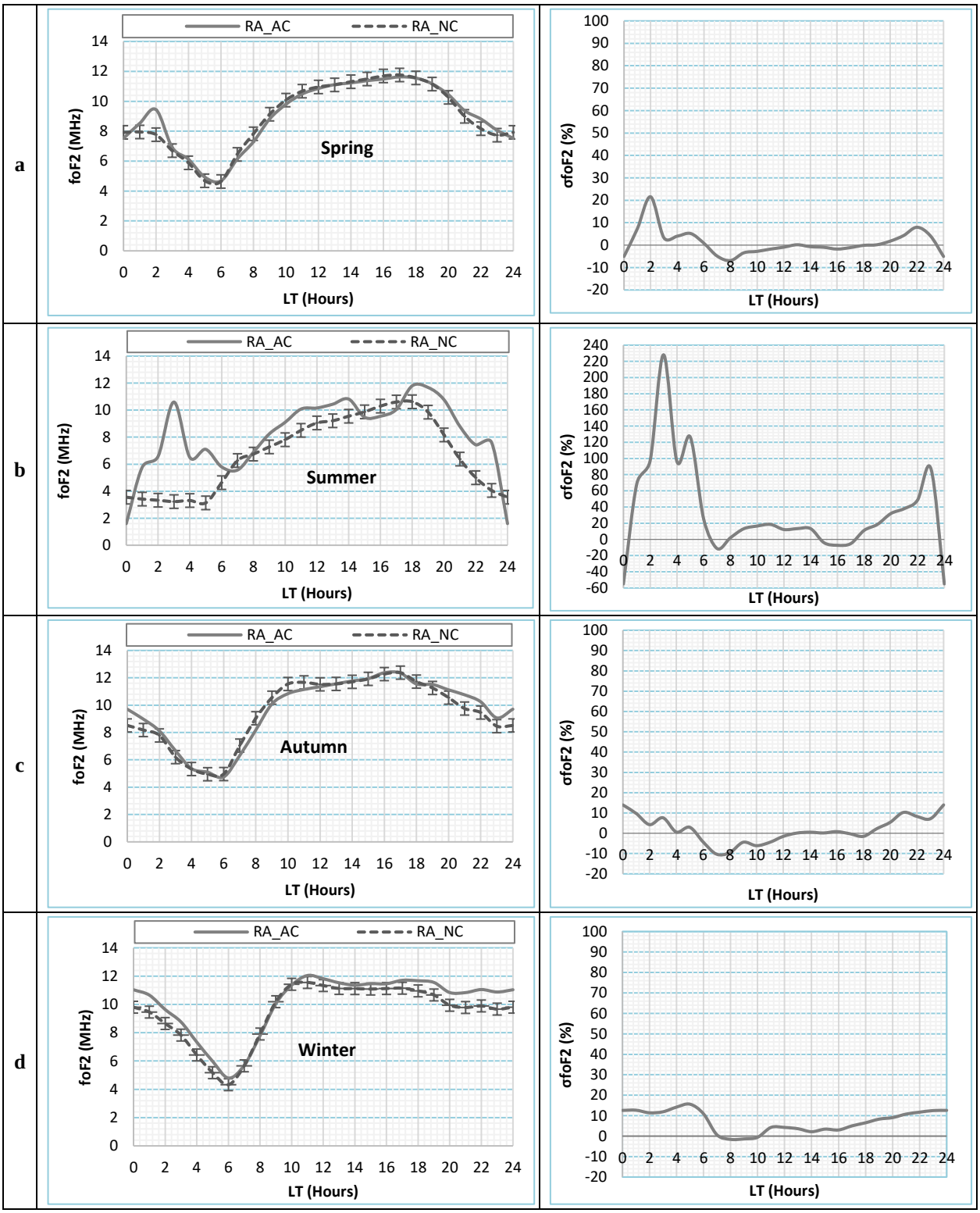

Figure 5:- foF2 diurnal variation during recurrent activity (RA) throughout spring (panel a), summer (panel "b"), autumn (panel "c") and winter (panel "d") seasons. The dashed curve is for the New classification (NC) and the solid one for the Ancient Classification (AC). The left column is devoted to the foF2 diurnal variation profiles and the right one presents the relative deviation percentage of foF2 between the RA foF2 values of the AC and that of the NC.

Figure 6 shows the foF2 values diurnal variation for the SA of the two classifications and the relative deviation percentage of foF2 diurnal values of both classifications. Panel "a" presents a "P" profile for the two curves during spring time. Therefore, the SA is characterised by a weak electrojet during spring season. Besides, we observe that the two curves present the same shape and the same amplitude with respect to error bars shown in NC graph. In fact, the right column of this panel highlight that the σfoF2 value is within $\pm 10\%$ between all the daily times; thus, the shock events foF2 daily profiles variation of both classifications are in good agreement during spring time. The maximum negative value of σfoF2, equals to -6.22%, is observed at 0400 LT and the maximum positive value is observed at 0200 LT and it is equal to +4.3%.

In panel "b" we observe that both graphs present a "D" profile which highlights the signature of an absence of electrojet during summer time for 2 classification's SA. Otherwise, the AC graph is always above that of the NC; the two classification's graphs are different between 1300 LT to 1700 LT and 2100 LT to 0400 LT with respect to error bars shown in NC graph. Besides, the right column of this panel highlights a σfoF2 value greater than +10% between 2100 LT to 0400 LT and a value within $\pm 10\%$ the time remaining. The maximum positive value is observed at 0000 LT and it is equal to $+68.53\%$.

Panel "c" shows a "B" profile with a lower trough at 1200 LT for both curves. Therefore, the 2 classification's SA are characterised by a short living high electrojet located at 1200 LT during autumn time. Otherwise, the AC graph is always down that of the NC; the two classifications are different during a meantime surrounding 0100 LT and 0300 LT with respect to error bars shown in NC graph. Besides, the right column of this panel highlights a σfoF2 value negative all the daily time with values small than -10% at 0100 LT and at 0300 LT and values within $\pm 10\%$ the time remaining. The maximum negative value is observed at 0300 LT and it is equal to -12.67% and the maximum positive value, equal to $+0{,}35\%$ is observed at 2100 LT.

Panel "d" shows an "M" profile for both classifications curves. Therefore, the 2 classification's SA are characterised by a moderate electrojet during winter time. Otherwise, we observe that the AC graph is almost always above that of the NC, except between 0900 LT to 1100 LT. The two classifications are different between 0400 LT to after 0600 LT with respect to error bars shown in NC graph. Besides, the right column of this panel highlights negative value of σfoF2 between 0900 LT to 1100 LT and positive the time remaining. The maximum negative value of σfoF2, observed at 1000 LT, is equal to -1.08% and its maximum positive value, observed at 0600 LT, is equal to $+13.59\%$.

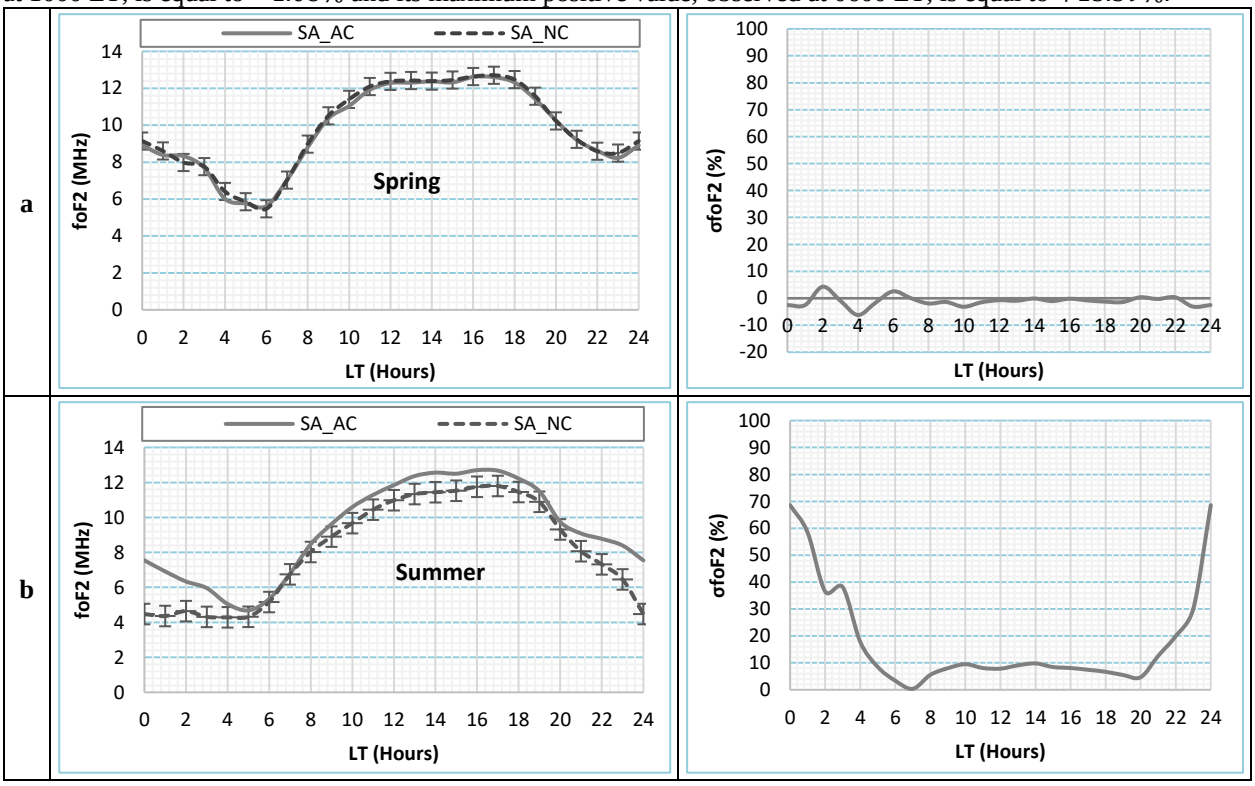

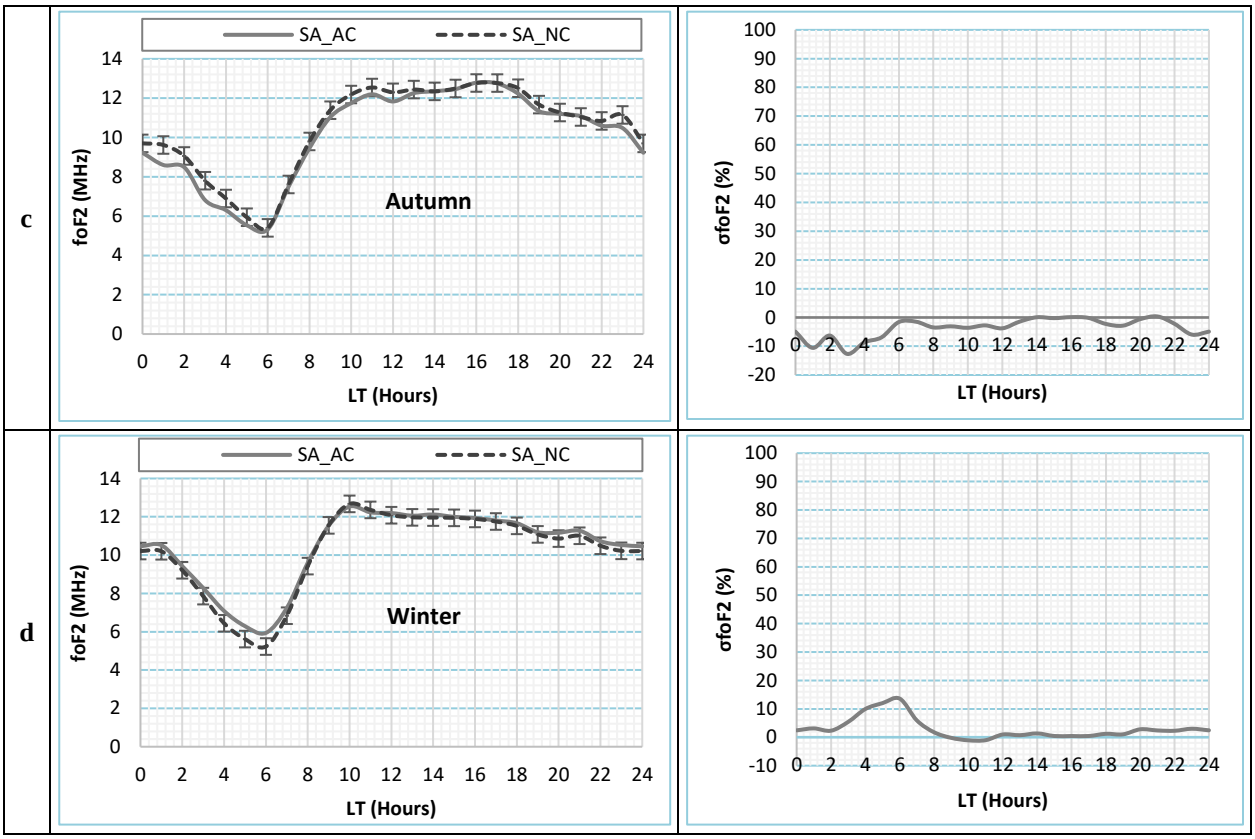

Figure 6:- The same as figure 5 but for shock activity.

Conclusion:-

This paper shows that both classification's geomagnetic classes, at Dakar station, are different in terms of occurrences throughout seasons. It emerges that the more the occurrences between two classes for a given season are different, the more the profiles show difference. Therefore, it's observed an obvious difference of the electrodynamics in the ionosphere layer during the disturbed geomagnetic activities according to both classifications method. In general the AC and NC curves show different profiles during the summer season for the RA and the SA. The FA profiles don't depend on the classification method at all.

Acknowledgments:-

The authors thank Brest Telecom of Bretagne for providing Dakar ionosonde data. Many thanks to ISGI data centre for providing data centre.

References:-

1. Abdu, M.A., Bittencourt, J.A., and Batista, I.S. (1981). Magnetic declination control of the equatorial F region dynamo electric field development and spread F. J. Geophys. Res. Space Phys. 86, 11443–11446.
2. Abdu, M.A., Batista, I.S., and Sobral, J.H.A. (1992). A new aspect of magnetic declination control of equatorial spread F and F region dynamo. J. Geophys. Res. Space Phys. 97, 14897–14904.
3. Acharya, R., Roy, B., Sivaraman, M.R., and Dasgupta, A. (2010). An empirical relation of daytime equatorial total electron content with equatorial electrojet in the Indian zone. J. Atmospheric Sol.-Terr. Phys. 72, 774–780.
4. Acharya, R., Roy, B., Sivaraman, M.R., and Dasgupta, A. (2011). On conformity of the EEJ based Ionospheric model to the Fountain effect and resulting improvements. J. Atmospheric Sol.-Terr. Phys. 73, 779–784.
5. Ali, M.N., Ouattara, F., Zerbo, J.-L., Gyébré, A.M.F., Nanema, E., and Zougmoré, F. (2015). Statistical Study of foF2 Diurnal Variation at Dakar Station from 1971 to 1996: Effect of Geomagnetic Classes of Activity on Seasonal Variation at Solar Minimum and Maximum. Int. J. Geosci. 6, 201.

6. Diabaté, A., Ouattara, F., and Zerbo, J.-L. (2018). Annual and Diurnal Variabilities in the Critical Frequency (foF2) during Geomagnetic Fluctuating Activity over Solar Cycles 21 and 22 at Ouagadougou. Atmospheric Clim. Sci. 8, 435–445.
7. Diabaté, A., Zerbo, J.L., and Ouattara, F. (2019). Variation of the foF2 parameter during fluctuating activity: Prediction with IRI-2012 compared to measured data from Ouagadougou inosonde station during solar cycles 21 and 22. Vietnam J. Earth Sci. 41, 59–68.
8. Dunford, E. (1967). The relationship between the ionospheric equatorial anomaly and the E-region current system. J. Atmospheric Terr. Phys. 29, 1489–1498.
9. Farley, D.T., Bonelli, E., Fejer, B.G., and Larsen, M.F. (1986). The prereversal enhancement of the zonal electric field in the equatorial ionosphere. J. Geophys. Res. Space Phys. 91, 13723–13728.
10. Faynot, J.M., and Vila, P. (1979). F region strata at the Magnetic Equator. Ann. Geophys. 35, 1–9,.
11. Fejer, B.G. (1981). The equatorial ionospheric electric fields. J. Atmospheric Terr. Phys. 43, 377–386.
12. Fejer, B.G., Farley, D.T., Woodman, R.F., and Calderon, C. (1979). Dependence of equatorial F region vertical drifts on season and solar cycle. J. Geophys. Res. Space Phys. 84, 5792–5796.
13. Fejer, B.G., Farley, D.T., Gonzales, C.A., Woodman, R.F., and Calderon, C. (1981). F region east-west drifts at Jicamarca. J. Geophys. Res. Space Phys. 86, 215–218.
14. Gnabahou, D.A., and Ouattara, F. (2012). Ionosphere variability from 1957 to 1981 at Djibouti station. Eur. J. Sci. Res. 73, 382–390.
15. Gnabahou, D.A., Ouattara, F., Nanéma, E., and Zougmoré, F. (2013). foF2 diurnal variability at African equatorial stations: Dip equator secular displacement effect. Int. J. Geosci. 4, 1145.
16. Guibula, K., Ouattara, F., and Gnabahou, D.A. (2018). foF2 Seasonal Asymmetry Time Variation at Korhogo Station from 1992 to 2002. Int. J. Geosci. 9, 207.
17. Guibula, K., Zerbo, J.-L., Kaboré, M., and Ouattara, F. (2019). Critical Frequency foF2 Variations at Korhogo Station from 1992 to 2001 Prediction with IRI-2012. Int. J. Geophys. 2019.
18. Gyébré, A.M.F., Gnabahou, D.A., and Ouattara, F. (2018). The Geomagnetic Effects of Solar Activity as Measured at Ouagadougou Station. Int. J. Astron. Astrophys. 8, 178.
19. Kaboré, M., Zerbo, J.-L., Zoundi, C., and Ouattara, F. (2019). Variability of the Critical Frequency foF2 for Equatorial Regions during Solar Cycle's Minima and Maxima at Ouagadougou and Manila Stations. Int. J. Geosci. 10, 833.
20. Legrand, J.-P., and Simon, P.A. (1989). Solar cycle and geomagnetic activity: a review for geophysicists. I-The contributions to geomagnetic activity of shock waves and of the solar wind. 7, 565–578.
21. Mayaud, P.N. (1971). Une mesure planétaire d'activité magnétique basée sur deux observatoires antipodaux. Ann Geophys 27, 67–70.
22. Mayaud, P.N. (1972). The aa indices: A 100-year series characterizing the magnetic activity. J. Geophys. Res. 77, 6870–6874.
23. Mayaud, P.N. (1973). A hundred year series of geomagnetic data, 1868-1967: indices aa, storm sudden commencements. IAGA Bull. 33, 256.
24. Mayaud, P.N. (1980). Derivation, meaning, and use of geomagnetic indices. Wash. DC Am. Geophys. Union Geophys. Monogr. Ser. 22.
25. Nanema, E., Gnabahou, D.A., Zoundi, C., and Ouattara, F. (2018). Modeling the Ionosphere during Quiet Time Variation at Ouagadougou in West Africa. Int. J. Astron. Astrophys. 8, 163.
26. Nanéma, E., and Ouattara, F. (2013). HmF2 quiet time variations at Ouagadougou and comparison with IRI-2012 and TIEGCM predictions during solar minimum and maximum. Arch. Appl. Sci. Res. 5, 55–61.
27. Nanéma, E., Konaté, M., and Ouattara, F. (2019). Peak of Electron Density in F2-Layer Parameters Variability at Quiet Days on Solar Minimum. J. Mod. Phys. 10, 302–309.
28. Ouattara, F. (2009). Relationship between geomagnetic classes' activity phases and their occurrence during the sunspot cycle. Ann. Geophys. 52, 107–116.
29. Ouattara, F. (2013). IRI-2007 foF2 predictions at Ouagadougou station during quiet time periods from 1985 to 1995. Arch. Phys. Res. 4, 12–18.
30. Ouattara, F., and Amory-Mazaudier, C. (2008). Solar–geomagnetic activity and Aa indices toward a Standard. Journal of Atmospheric and Solar-Terrestrial Physics 1736– 1748.
31. Ouattara, F., and Amory-Mazaudier, C. (2009). Solar–geomagnetic activity and Aa indices toward a standard classification. J. Atmospheric Sol.-Terr. Phys. 71, 1736–1748.
32. Ouattara, F., and Amory-Mazaudier, C. (2012). Statistical study of the equatorial F layer critical frequency at Ouagadougou during solar cycles 20, 21 and 22, using Legrand and Simon's classification of geomagnetic activity. EDP Sci. 2012 2.

33. Ouattara, F., and Nanéma, E. (2014). Quiet Time foF2 Variation at Ouagadougou Station and Comparison with TIEGCM and IRI-2012 Predictions for 1985 and 1990. Phys. Sci. Int. J. 892–902.
34. Ouattara, F., and Zerbo, J.-L. (2011). Ouagadougou station F2 layer parameters, yearly and seasonal variations during severe geomagnetic storms generated by coronal mass ejections (CMEs) and fluctuating wind streams. Int. J. Phys. Sci. 6, 4854–4860.
35. Ouattara, F., Amory-Mazaudier, C., Menvielle, M., Simon, P., and Legrand, J.-P. (2009). On the long term change in the geomagnetic activity during the 20th century.
36. Ouattara, F., Kaboré, S., Gyébré, A.M.F., and Zerbo, J.-L. (2015). CMEs' Shock Occurrences from Solar Cycle 11 to solar Cycle 23. uropean Journal of Scientific Research 130, 153–159.
37. Ouattara, F., Zerbo, J.-L., Kaboré, M., and Fleury, R. (2017). Investigation on equinoctial asymmetry observed in Niamey Station Center for Orbit Determination in Europe Total Electron Content (CODG TEC) variation during~ solar cycle 23. Int. J. Phys. Sci. 12, 308–321.
38. Richardson, I.G., Cliver, E.W., and Cane, H.V. (2000). Sources of geomagnetic activity over the solar cycle: Relative importance of coronal mass ejections, high-speed streams, and slow solar wind. J. Geophys. Res. Space Phys. 105, 18203–18213.
39. Richardson, I.G., Cliver, E.W., and Cane, H.V. (2001). Sources of geomagnetic storms for solar minimum and maximum conditions during 1972–2000. Geophys. Res. Lett. 28, 2569–2572.
40. Richardson, I.G., Cane, H.V., and Cliver, E.W. (2002). Sources of geomagnetic activity during nearly three solar cycles (1972–2000). J. Geophys. Res. Space Phys. 107, SSH 8–1–SSH 8–13.
41. Sawadogo, W.E., Zerbo, J.-L., Ali, M.N., and Ouattara, F. (2019a). Diurnal variation of F2-layer critical frequency under solar activity recurrent conditions during solar cycles 21 and 22 at Ouagadougou Station: Prediction with IRI-2012. Sci. Res. Essays 14, 111–118.
42. Sawadogo, W.E., Ouattara, F., and Ali, M.N. (2019b). The Effects of the Recurrent Storms on Fof2 at Ouagadougou Station during Solar Cycles 21-22. Int. J. Geosci. 10, 80.
43. Simon, P.A., and Legrand, J.P. (1989). Solar cycle and geomagnetic activity: a review for geophysicists. Part 2. The solar sources of geomagnetic activity and their links with sunspot cycle activity. Annales Geophysicae 7, 579–594.
44. Svalgaard, L. (1977). Geomagnetic activity: dependence on solar wind parameters. (STANFORD UNIV CALIF INST FOR PLASMA RESEARCH).
45. Thiam, N., Ouattara, F., Gnabahou, A., Amory Mazaudier, C., Fleury, R., and Duchesne, P.L. (2012). Variation de la Fréquence Critique de la Couche F2 (foF2) de la Station de Dakar avec le Cycle Solaire. J. Sci. 11, 16–20.
46. Vassal, J. (1982a). Electrojet, contre-électrojet et région F à Sarh (Tchad). Géophysique 3–9.
47. Vassal, J. (1982b). La variation du champ magnétique et ses relations avec I'électrojet équatorial au Sénégal Oriental. Ann Geophys 38, 347–355.
48. Zerbo, J.-L., Ouattara, F., Zoundi, C., and Gyébré, A.M.F. (2011). Solar cycle 23 and geomagnetic activity since 1868. Rev. CAMES Sér. A 12, 255–262.
49. Zerbo, J.-L., Amory Mazaudier, C., Ouattara, F., and Richardson, J.D. (2012). Solar wind and geomagnetism: toward a standard classification of geomagnetic activity from 1868 to 2009. Annals of Geophysics 30, 421–426.
50. Zerbo, J.-L., Ouattara, F., Amory-Mazaudier, C., Legrand, J.-P., and Richardson, J.D. (2013). Solar activity, solar wind and geomagnetic signatures. Atmospheric and Climate Science 3, 610–617.